UNIVERSITY OF
BATH

University of Bath

ARTICLE TYPE

Crystallisation and physicochemical property characterisation of conformationally-locked co-crystals of fenamic acid derivatives

K. E. Wittering,[a,b] L. R. Agnew,[a,b] A. R. Klapwijk,[a,b] K. Robertson,[a,b] A. J. P. Cousen,[a,b] D. L. Cruickshank[*a] and C. C. Wilson[*a,b]

Polymorphism in drug compounds can cause significant problems for industrial-scale production and so a method for restricting the conformational freedom of the target compound whilst retaining desired chemical properties is highly beneficial to the pharmaceutical industry. Co-crystallisation is commonly
10 used to alter the structure of an active pharmaceutical ingredient (API) without affecting its activity. A comprehensive co-crystal screen of four fenamic acid derivatives affords a strictly limited number of co-crystals. These show no evidence of polymorphism, although some of the parent APIs exhibit significant polymorphism. Two of these co-crystals, of mefenamic acid and tolfenamic acid with 4,4'-bipyridine, were previously unknown and are studied using X-ray diffraction. Co-crystals from this screen are fully
15 characterised and display comparable solubility and stability with respect to the parent APIs; no phase transformations have been identified. A range of crystallisation techniques, including cooling and grinding methods, are shown to afford single polymorphic forms for each of the co-crystals.

Introduction

Fenamic acid (FEN) and its derivatives are a well-known class of
20 non-steroidal anti-inflammatory drugs (NSAIDs) that have been studied extensively in the solid state. Flufenamic acid (FLU), mefenamic acid (MEF) and tolfenamic acid (TOL) (Fig. 1), which are the subject of this paper, have previously been shown to exhibit conformational polymorphism; this is manifested particularly in
25 FLU which has nine reported polymorphs.[1-4] This polymorphic nature can be attributed to the torsional freedom of the amine functionality positioned between the two phenyl rings. The amine group can form an intramolecular hydrogen bond with the carboxylic acid group on the adjacent phenyl ring, common to all
30 derivatives, which locks this half of the molecule into a planar geometry. Meanwhile the other half, a second phenyl ring, has torsional freedom which is influenced by the functional groups present.
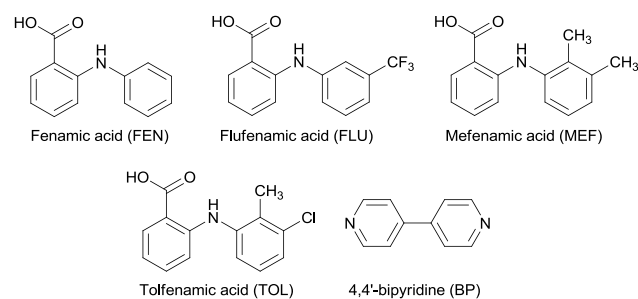
35 **Fig. 1** Chemical structures of fenamic acid derivatives and the co-former 4,4'-bipyridine

It is vital to understand polymorphism in materials, notably active pharmaceutical ingredients (APIs), as the variation in solid state packing can have a profound effect upon physicochemical
40 properties of the solid form such as solubility and stability.[5-7] There are several possible routes to obtain a desired solid form; this includes use of specific crystallisation techniques (such as hot melt extrusion[8], spray drying[9] and cooling crystallisation[10]), or through crystallisation with additives. The term additive encompasses both
45 size-matched components and polymers that are used to influence the crystallisation process without integration into the crystal structure.[1,4,11] Lee and co-workers have demonstrated templating of metastable MEF form II using FLU as an additive.[12] Multi-component materials can provide an alternative route to solid form
50 control through the formation of either solvates, hydrates, salts or co-crystals.[13] Similar to polymorphism, these types of compounds can also have improved physicochemical properties whilst retaining the activity of the API. Co-crystals are the focus of the presented work.

55 There are a limited number of known salts of fenamic acid derivatives and even fewer examples of co-crystals (multi-component molecular crystals in which no proton transfer has occurred between the API and co-former, leaving both components neutral). Reported salts include MEF with a range of
60 alkanolamines[14] as well as tetraazacyclododecane, tetraazacyclotetradecane and tris(hydroxymethyl)-aminomethane.[15] Previously reported co-crystals of the fenamic acid series contain co-former molecules that are dominated by cyclic amines including nicotinamide, 4,4'-bipyridine, pyridine, 2-
65 aminopyridine, 4-aminopyrazine and piperazine.[16-19]

This study aims to discover whether co-crystallisation of

fenamates can afford enhanced polymorphic stability whilst achieving solubility and chemical stability comparable to the target compound. The fenamate family provides ideal target candidates due to the high level of polymorphism exhibited by this class of
5 molecules. The different polymorphs can exhibit variation in solid form properties and so are unfavourable for their scale-up into optimised production processes. A thorough co-crystal screen, which involved co-crystallisation of the four fenamic acid derivatives with a wide range of second components (co-formers)
10 in an array of solvents, was used to investigate the variety of co-crystals accessible. This is important in order to develop a robust industrial crystallisation process where there is a single solid form product with comparable physical properties to that of the desired polymorph of the target API. There is no evidence in the
15 Cambridge Structural Database (CSD)[20] of fenamate co-crystals involving hydrogen bonding of carboxylic acid groups from disparate molecules. The interaction of the carboxylic acid groups between two fenamic acid derivatives appears to be too strong to be disrupted by the carboxylic acid functionality of a co-former.
20 Therefore the co-formers investigated were predominantly selected as they contain basic nitrogen atoms and these have been shown to interact with the carboxylic acid groups of fenamates.[14-19]

Solubility and stability of two previously reported co-crystals of
25 FLU[17] and FEN[19] with 4,4'-bipyridine (BP) are presented in this study along with two co-crystals of TOL and MEF with BP[‡] which were identified during our co-crystal screening process. Solubility data for the starting materials are also included here, as the solvent systems used in this study differs from those previously
30 reported.[12,17] Despite 4,4'-bipyridyl being a non-GRAS (Generally Recognised as Safe) molecule, it was utilised as a very common co-former which lends itself to hydrogen bonding due to the basicity of the ring-bound nitrogen.[22]

To our knowledge the co-crystals reported herein have
35 previously been produced only through evaporative or grinding methods. In the interest of scale-up and optimisation for industrial crystallisation, we present here the successful co-crystallisation of a series of fenamates with BP *via* cooling crystallisation. The optimisation of crystallisation within a cooling environment is of
40 particular importance as the majority of industrial crystallisation processes are achieved through this technique[23,24] either in batch cooling crystallisation using stirred tank reactors or continuous crystallisation processes.

Experimental

45 MEF, FLU, FEN and BP were purchased from Sigma Aldrich Chemie Gmbh (Steinheim, Germany) and TOL was purchased from TCI UK Ltd (Oxford, UK). All reagents were used without further purification. Laboratory grade solvents purchased from Sigma Aldrich were used for all crystallisations.

50
Evaporative crystallisation
Thorough co-crystal screening studies were conducted through

evaporative crystallisation methods using several different GRAS co-former molecules, solvents, ratios of API:co-former and
55 crystallisation temperatures (*ca.* 300 crystallisations, variables detailed in Table S1†). Powder X-ray diffraction was initially used to screen all samples for the presence of new co-crystals. This led to the identification of two initially unknown[‡] co-crystals which were structurally characterised using single crystal X-ray
60 diffraction after single crystals of suitable quality were obtained through evaporative crystallisation methods; the previously reported structure of FLU-BP was also re-determined. The following evaporative conditions were used to produce the four co-crystals characterised in this investigation:
65 **FEN-BP.** Pale brown crystals were obtained by dissolving ca. equimolar quantities of FEN (26 mg, 0.12 mmol) and BP (20 mg, 0.12 mmol) in a minimal volume of ethanol. The solution was left to evaporate at room temperature.
FLU-BP. Bright yellow needle-like crystals were obtained within
70 24 hours after dissolving *ca.* equimolar quantities of FLU (30 mg, 0.12 mmol) and BP (17 mg, 0.11 mmol) in a minimal volume of methanol and leaving the solvent to evaporate at room temperature.
MEF-BP. Equimolar quantities of MEF (30 mg, 0.12 mmol) and BP (20 mg, 0.12 mmol) were placed into a vial and dissolved in a
75 minimal volume of isopropanol (IPA). Holes were pierced in the lid to allow for slow evaporation at 4 °C. After two days single crystals (pale yellow blocks) were present in solution.
TOL-BP. Equimolar quantities of TOL (30 mg, 0.11 mmol) and BP (18 mg, 0.11 mmol) were dissolved in a minimal volume of
80 acetone. The solution was left at room temperature to evaporate slowly and yellow needle-like crystals were observed after 24 hours.

Liquid-assisted grinding
85 All samples used for the solubility and stability measurements were prepared by kneading a 2:1 molar ratio of the API to BP with a pestle and mortar for 15 minutes with drop-wise addition of ethanol and IPA for the FEN-BP and MEF-BP co-crystals, respectively, and methanol for the FLU-BP and TOL-BP co-
90 crystals. Powder X-ray diffraction (PXRD) was used to confirm that the solid forms of the kneaded samples were the same as those obtained from the slow evaporation method (see Fig. S1†).

Cooling crystallisation
All co-crystals resulting from the evaporative screens were also
95 produced using two different cooling procedures; a rapid cooling method and a controlled linear cooling route detailed below. The quantities of the co-crystal components were initially based on the solubility data obtained for the individual APIs in an IPA/H$_2$O solvent system. Although this method was successful for FEN-BP,
100 this proved unsuccessful for FLU-BP producing a physical mixture of the individual components and very low yields of the MEF-BP and TOL-BP co-crystals. The molar ratios were therefore adjusted until the desired co-crystals could be produced reproducibly. Furthermore, in order to maximise the yield obtained for MEF-BP

[‡] While the present manuscript was in its first stage of revision, Surov *et al.* in parallel synthesised and determined the X-ray crystal structures of TOL-BP and MEF-BP co-crystals.[21]

and TOL-BP the solvent system was changed to IPA and ethanol respectively.

Rapid cooling

FEN-BP. Equimolar quantities of FEN (35 mg, 0.16 mmol) and BP (26 mg, 0.17mmol) were dissolved in 5 g of IPA/H_2O (1:1 v/v) in a 10 ml glass vial, to produce a solution saturated with respect to FEN. Once dissolved the solution was rapidly cooled in an ice bath to yield pale brown crystalline needles.

FLU-BP. A solution of FLU (50 mg, 0.18 mmol) and BP (14 mg, 0.09 mmol) was prepared using 5 g of IPA/H_2O (1:1 v/v) to give a 2:1 (FLU:BP) solution saturated with respect to FLU. After dissolution the solution was rapidly cooled in an ice bath which produced bright yellow crystalline needles.

MEF-BP. Equimolar quantities of MEF (75 mg, 0.31 mmol) and BP (49 mg, 0.31 mmol) were dissolved in 5 g of IPA in a 10 ml glass vial, to produce a solution saturated with respect to MEF. Subsequently the solution was rapidly cooled in an ice bath to produce a pale yellow polycrystalline powder.

TOL-BP. TOL (150 mg, 0.57 mmol) and BP (60 mg, 0.38 mmol) were dissolved in 5 g of ethanol in a 10 ml glass vial, to give a solution saturated with respect to TOL in a 3:2 molar ratio (TOL:BP). This solution was rapidly cooled in an ice bath to give a pale yellow polycrystalline powder.

Controlled linear cooling

The components were placed in 10 ml vials to which 5 g of solvent was added. The chosen solvent and respective masses of the starting materials used were the same as for the rapid cooling experiments. These vials were subjected to a linear cooling profile of 50 °C to 5 °C at 0.05 °C min⁻¹ using the Cambridge Reactor Design Polar Bear Plus crystalliser. Magnetic bottom stirring was used to obtain a stirring rate of 300 rpm.

Single crystal X-ray diffraction. X-ray diffraction data were recorded on an Agilent Technologies Gemini A Ultra CCD diffractometer, using monochromatic Mo-K$_\alpha$ radiation ($\lambda = 0.71073$ Å) at 150 K. The sample temperature was controlled using an Oxford Diffraction Cryojet apparatus and the data processed using CrysAlisPro version 1.171.36.21. The structures were solved by direct methods using SHELXS-97 and full matrix least-squares refinement was carried out using SHELXL-97.[25] All non-hydrogen atoms were refined anisotropically and the hydrogen atoms were placed based on the Fourier difference maps. Molecular parameters for all structures were computed using the program PLATON.[26] Crystallographic data and refinement parameters confirmed the known structures of all complexes, including the very recently reported MEF-BP and TOL-BP (Table S2†).[21]

Powder X-ray diffraction. PXRD patterns were collected in flat plate mode on a Bruker D8 Advance equipped with monochromated Cu-K$_\alpha$ radiation ($\lambda = 1.54056$ Å) in reflection geometry at 298 K.

Thermal analysis. Differential scanning calorimetry (DSC) studies were carried out using a Thermal Advantage Q20 DSC from TA Instruments, equipped with Thermal Advantage Cooling System 90 and operated with a dry nitrogen purge gas at a flow rate of 18 cm³ min⁻¹. The samples were placed in sealed Tzero aluminium pans and a heating/cooling rate of 10 K min⁻¹ was used. Data were collected using the software Advantage for Qseries.[27] Complementary visual characterisation of the thermal properties of the co-crystals was carried out using a Mettler Toledo FP82 hot stage equipped with a Leica DM1000 microscope. Each crystal was subjected to a programmed temperature regime using the FP90 Central Processor. The crystals were filmed using an Infinity 2 microscopy camera.

Relative humidity studies. Samples of the BP co-crystals, prepared by liquid-assisted grinding, and their corresponding fenamic acid starting materials were stored under moderate (24 °C and 45% relative humidity) and harsh (45 °C and 80% relative humidity) humidity conditions for a four and two week period respectively. Samples were taken at regular intervals and analysed using PXRD to determine the stability of the materials under these conditions with time.

Infrared spectroscopy. The FTIR spectra were recorded at room temperature using a Perkin Elmer FTIR Spectrometer in the range 4000-500 cm⁻¹ with an ATR sampling accessory.

Solubility measurements. Solubility studies were carried out in a mixed solvent system of IPA and water (1:1 v/v) using a CrystallinePV parallel crystalliser from Technobis Crystallization Systems BV (formerly Avantium Pharmatech BV). Comprised of eight individually controlled reactors each with a working volume of 3-8 cm³, the CrystallinePV couples turbidity measurements with in-line particle visualisation and was used to obtain the necessary solubility information. The combination of turbidimetric data and images from in-line cameras allows determination of clear points with improved accuracy over turbidity measurements alone. Vials were cycled through temperature ranges from 20 °C to 75 °C using a heating rate of 0.5 K min⁻¹ and stirring at 800 rpm using standard (4 mm) magnetic stirrer bars. Data were analysed using CrystalClear software.[28] It should be noted that this solvent system is generally regarded as acceptable for deployment in crystallisation processes within the pharmaceutical industry.

Results and Discussions

Solid-state structures

The two recently reported co-crystals, also initially discovered in parallel in this study (MEF-BP and TOL-BP) as well as the previously reported complexes FEN-BP and FLU-BP can be prepared through evaporative methods, cooling methods and by liquid-assisted grinding. A range of other GRAS co-formers were explored; however no new pharmaceutically relevant co-crystals were prepared. The scarcity of co-crystals of fenamic acid derivatives, as reported in this study and in previous literature, is due to both the strong carboxylic acid homodimer synthon that is dominant within the numerous polymorphs of the fenamic acid derivatives, and the ability for the molecules to adopt several stable conformations of their own. The strength of these interactions within these systems results in the evident preferential formation of polymorphs over co-crystals. Observations on the structures and
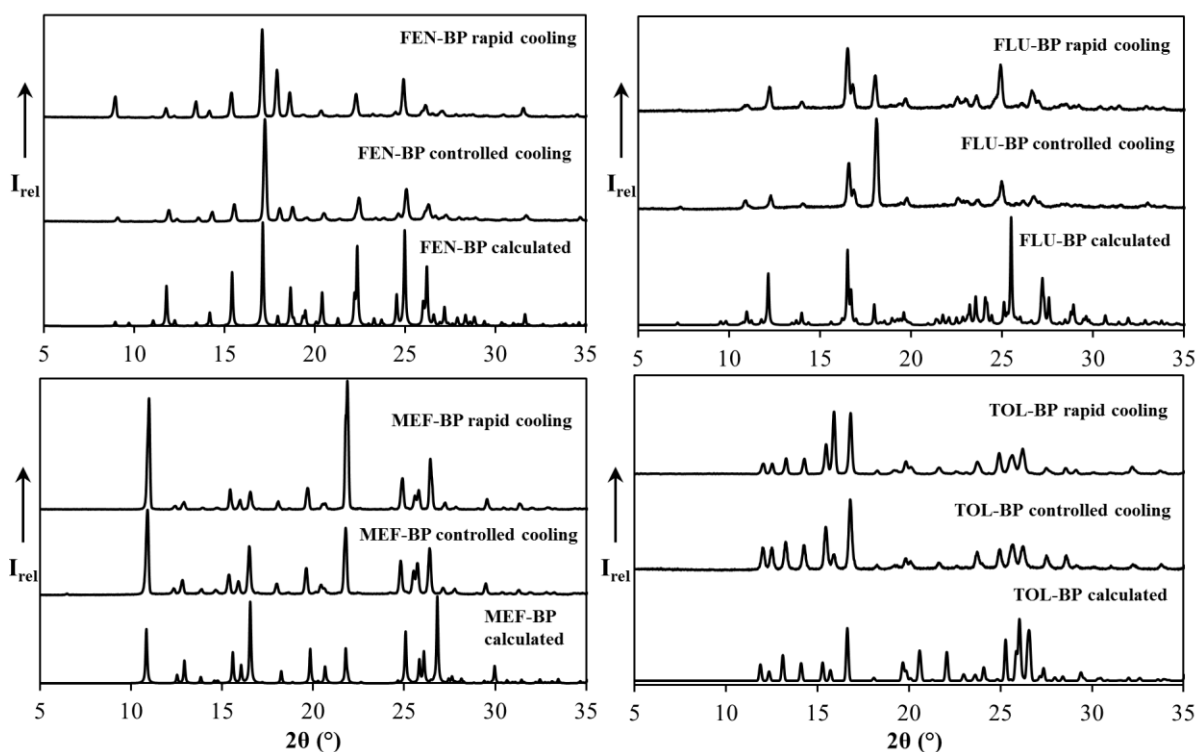
Fig. 2 Experimental PXRD patterns of the co-crystals from rapid and controlled cooling crystallisation experiments and comparison with their calculated patterns

intermolecular interactions of these systems are given in the ESI, the most significant being:

- 2:1 API:BP complexes of all the co-crystals contain the common acid-pyridine hydrogen bonded heterosynthon and intramolecular N-H···O hydrogen bond (Fig. S2, Table S3†).

- the conformations of the molecules differ (Fig. S3 and S4†), and are affected by hydrogen bonding and π-π stacking– these conformational preferences can have an effect on reducing the polymorphic propensity of the complexes.

The co-crystalline products of FLU-BP, MEF-BP and TOL-BP prepared through the evaporative crystallisation method were analysed using PXRD for comparison with patterns calculated from the respective single crystal X-ray diffraction data (Fig. S1†). The peak positions and peak intensities of the experimental patterns match those of the computed patterns thus indicating that the single crystal used for structure determination is representative of the bulk material and contained no excess starting material.

Cooling Crystallisation

All samples obtained from the rapid cooling and controlled cooling crystallisations were analysed using PXRD (Fig. 2) and show that all four co-crystals can be reproducibly prepared on this scale. Interestingly, both the rapid cooling profile and the controlled cooling profile (0.05 °C min⁻¹) give the same crystalline form which may be an indication of the favourability and stability of these fenamate BP co-crystals.

Thermal analysis

A heat-cool cycle was carried out using DSC for each of the co-crystals and their corresponding APIs (Figs 3 and 4). Hot-stage microscopy (HSM) was also used to visualise the thermal event of melting for the co-crystals and to observe any other obvious phase changes upon heating or cooling (Fig. 5).

The DSC trace of FEN shows a single endothermic peak at 186 °C upon heating and two exothermic peaks at 116 and 106 °C upon cooling. FLU also displays one endothermic peak at 135 °C which corresponds to the melting point of the most stable polymorphic form of flufenamic acid. Both FEN and FLU decompose upon heating and thus the recrystallisation peaks seen for FEN could be assigned to decomposition products. The co-crystals of FEN and FLU with BP melt at lower temperatures (146 and 128 °C) than their free acids and recrystallise upon cooling at 116 and 107 °C respectively (Fig. 3).

The DSC trace of MEF shows an endothermic peak at 170 °C which corresponds to an enantiotropic phase transition of form I to form II.[2, 29, 30] This is followed by another endothermic peak at 231 °C which represents the melting point of MEF form II. Upon cooling an exothermic peak is observed at 135 °C which could be attributed to the recrystallisation of form I, which is stable at lower temperatures.[2] The DSC traces for TOL form I and form II both show a sharp endotherm at 213 °C which agrees with previously reported results.[4] Upon cooling, an exothermic peak is observed at 135 °C for form I and 150 °C for form II.
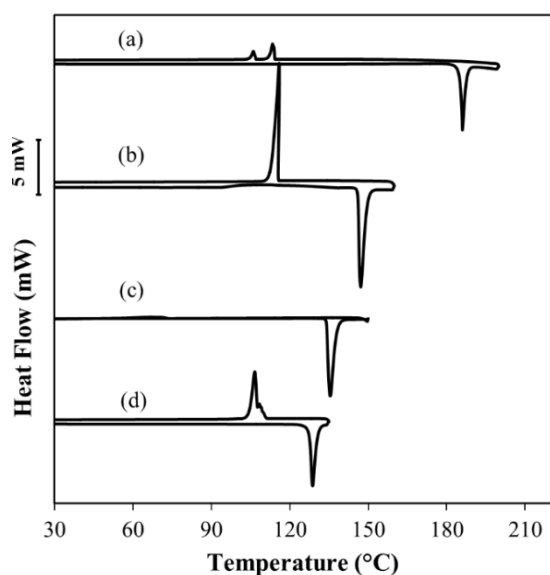
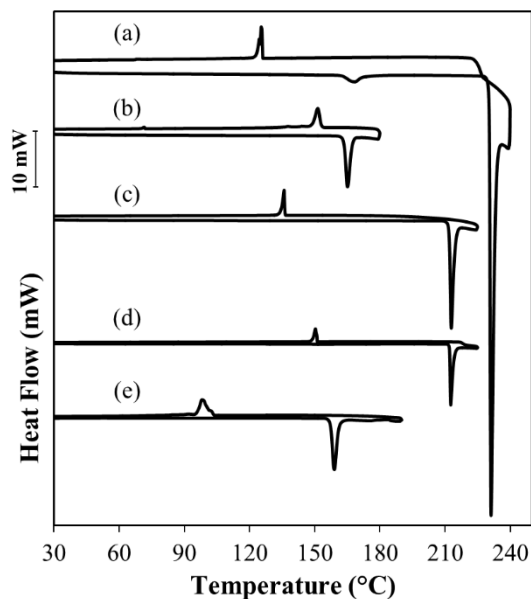**Fig. 3** Heat-cool DSC traces of a) FEN, b) FEN-BP, c) FLU and d) FLU-BP

Fig. 4 Heat-cool DSC traces of a) MEF (the y-component has been multiplied by three to clearly show the phase transition at 170 °C), b) MEF-BP, c) TOL Form I, d) TOL Form II and e) TOL-BP

The DSC profiles of MEF-BP and TOL-BP display endothermic peaks at 163 and 156 °C upon heating and exothermic recrystallisation peaks at 151 and 98 °C upon cooling (Fig. 4). In contrast to the DSC profile for FEN-BP and FLU-BP, where it can convincingly be stated that the co-crystals recrystallise upon cooling (owing to similar enthalpy changes for the endotherm and exotherm); the asymmetric and smaller exotherms for the other two co-crystals suggests a more complex thermal event than a simple recrystallisation of the co-crystal. These results are consistent with the events observed in the HSM images whereby the recrystallisation process is clearly evident upon cooling for the FEN and FLU co-crystals but not for the MEF-BP and TOL-BP samples (Fig. 5).
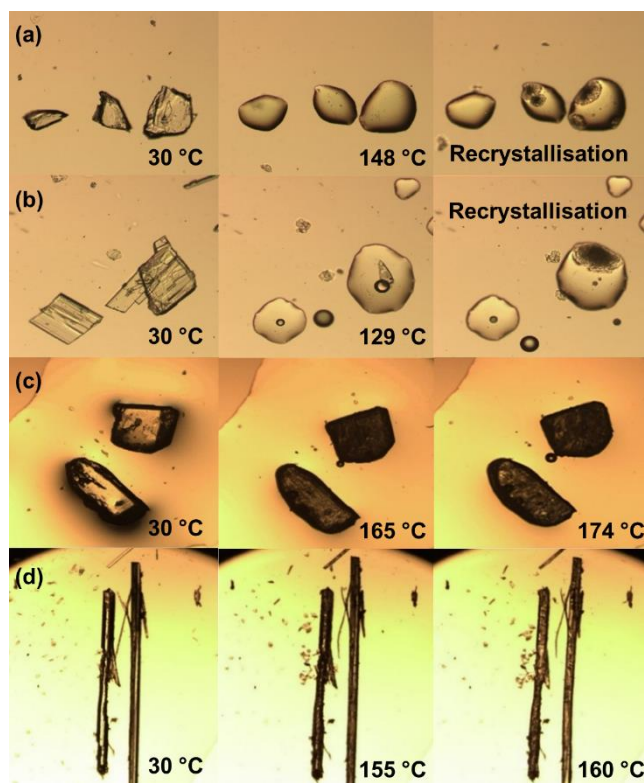

Fig. 5 HSM images illustrating the crystal morphologies of the BP co-crystals and their melts. a) FEN-BP and b) FLU-BP show evidence of recrystallisation upon cooling while c) MEF-BP and d) TOL-BP do not.

As many of the polymorphs of the fenamic acid derivatives differ only in a slight conformational change they have very similar melting points; the MEF form I to form II enantiotropic transition is an exception to this statement. It is common for phase transitions to be seen in DSC traces of polymorphic pharmaceuticals and it is therefore significant that in the DSC traces of these co-crystals there are no additional endothermic or exothermic peaks prior to melting that can be associated with a typical phase transition.

Furthermore, no polymorphs of the co-crystals were observed during the extensive co-crystal screen; this suggests locking of the conformational freedom on formation of the co-crystal structures has resulted in a reduction in the propensity for polymorphism in these fenamic acid derivatives.

The melting points of all of the co-crystals are significantly lower than those of their corresponding API, with the largest difference of *ca.* 66 °C between the melting point of the MEF-BP co-crystal and that of polymorphic form II of MEF (Table S4†).

IR spectra

Fourier Transform infrared spectroscopy was used to study the conformational and structural changes of the important functional groups involved in the hydrogen bonds. In the free acids, the carboxylic acid groups form standard $R_2^2(8)$ dimers (Fig. 6 a). In contrast, the co-crystals contain pyridine-acid supramolecular synthons and thus the carbonyl groups are not directly involved in the intermolecular hydrogen bonds and instead form a stronger intramolecular hydrogen bond with the secondary amine of the fenamic acids (Fig. 6 b).
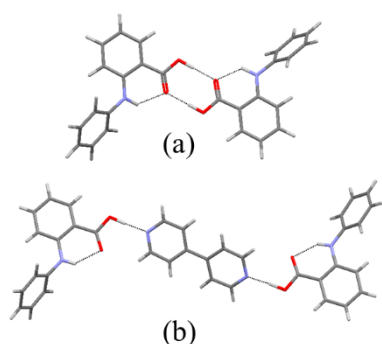
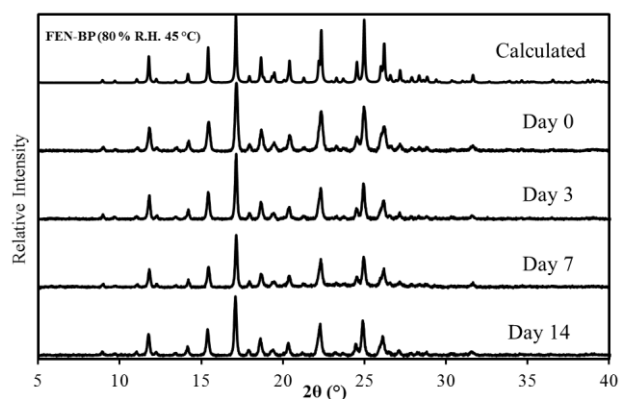**Fig. 6** Hydrogen bonding synthons present in a) pure fenamates and b) co-crystals

Detailed FTIR studies have been conducted on MEF form I and form II. It has been shown that form I, which contains the intramolecular hydrogen bond has an N-H stretching mode that occurs at a lower frequency (3311-3312 cm^{-1}) than form II (3346-3347 cm^{-1}) in which the intramolecular hydrogen bond no longer exists.[31] In all our results we see a redshift for the N-H stretching mode upon co-crystal formation indicating a strengthening of the intramolecular hydrogen bond. The C=O stretching mode undergoes a blueshift upon co-crystal formation, which is further supported by a decrease in the carbonyl bond length (Table 1). The dimeric hydrogen-bonded units that are commonly seen for the stable polymorphs of the fenamic acid derivatives have carbonyl stretching modes that occur at marginally lower frequencies than the co-crystals due to the increased C=O bond length which is due to a slight pull from the hydrogen bond acceptor. The large shifts (between 10 and 53 cm^{-1}) observed for the relevant stretching modes within these systems confirms the formation of co-crystals (Fig. S5†).

Table 1 Vibrational frequencies and bond lengths of selected functional groups partaking in hydrogen bonding for both the free fenamic acid derivatives and new co-crystals

Vibration frequency (cm^{-1})	FEN	FEN-BP	FLU	FLU-BP
N-H stretch	3334	3286	3320	3293
C=O stretch	1653	1666	1651	1671
C=O bond length (Å)	1.233	1.214	1.234	1.220
Vibration frequency (cm^{-1})	MEF	MEF-BP	TOL (I)/(II)	TOL-BP
N-H stretch	3308	3285	3339/3322	3286
C=O stretch	1647	1670	1654/1659	1664
C=O bond length (Å)	1.232	1.219	1.234/1.241	1.221

Relative humidity studies

A number of APIs are known to interconvert between polymorphic forms as well as anhydrous and monohydrate forms under relatively mild humidity conditions. This can cause serious issues with production, storage and transport of pharmaceutical products, and it has been shown that co-crystal formation of APIs can reduce or eliminate the possibility of these undesirable transformations.[32-35] The co-crystals of the fenamic acid derivatives studied here, along with the API starting materials, were thus investigated under

Fig. 7 PXRD patterns from the FEN-BP humidity study conducted at 80 % RH and 45 °C

moderate humidity storage conditions (24 °C and 45 % RH) and 'stress' humidity storage conditions (45 °C and 80 % RH) over a period of four and two weeks, respectively. PXRD patterns were recorded at various intervals and remained unchanged showing no indication of either new products being formed (possible hydrates) or dissociation of the co-crystals into their individual components (Fig. 7, Fig. S6† and Fig. S7†). These types of transformations normally occur at the higher humidity conditions (>75 % RH) and have been found to be dependent on the aqueous solubility of the two components.[35, 36] The fenamic acid derivatives investigated herein, however, are not known to form hydrates and have a low aqueous solubility thus the likelihood of the co-crystals dissociating at higher humidity conditions is low.

Solubility measurements

The solubilities of all four co-crystals and their corresponding API starting materials have been determined and compared. When evaluating the solubility of the raw starting materials, FLU is found to be more soluble than the other fenamic acid derivatives (5 mg g^{-1} at 25 °C) while MEF and TOL have very low solubilities in the IPA and water solvent system used. The new co-crystals of each fenamic acid derivative also follow this trend with the FLU-BP complex possessing the highest solubility.

Figure 8 shows the determined solubilities for each of the four target materials, and the comparison with that for their corresponding BP co-crystal. These results show that the solubility of the co-crystals is comparable to that of the parent APIs. It is important to note that these values only take into account the mass of the API within the co-crystal, allowing direct comparison with the solubility of the pure API.

Upon rapid cooling of a saturated solution of TOL, yellow needles of TOL form II were produced in sufficient quantity to allow the solubility of this polymorphic form to be determined in addition to that of TOL form I.

Conclusions

This work reports the co-crystal screening of a series of fenamic acid derivatives. A total of four co-crystals were discovered from these screens, two of which have been previously known and two discovered in parallel in this work and in a recent report.[21] These four co-crystals of fenamic acid, flufenamic acid, mefenamic acid and tolfenamic acid with the co-former 4,4'-bipyridine have been
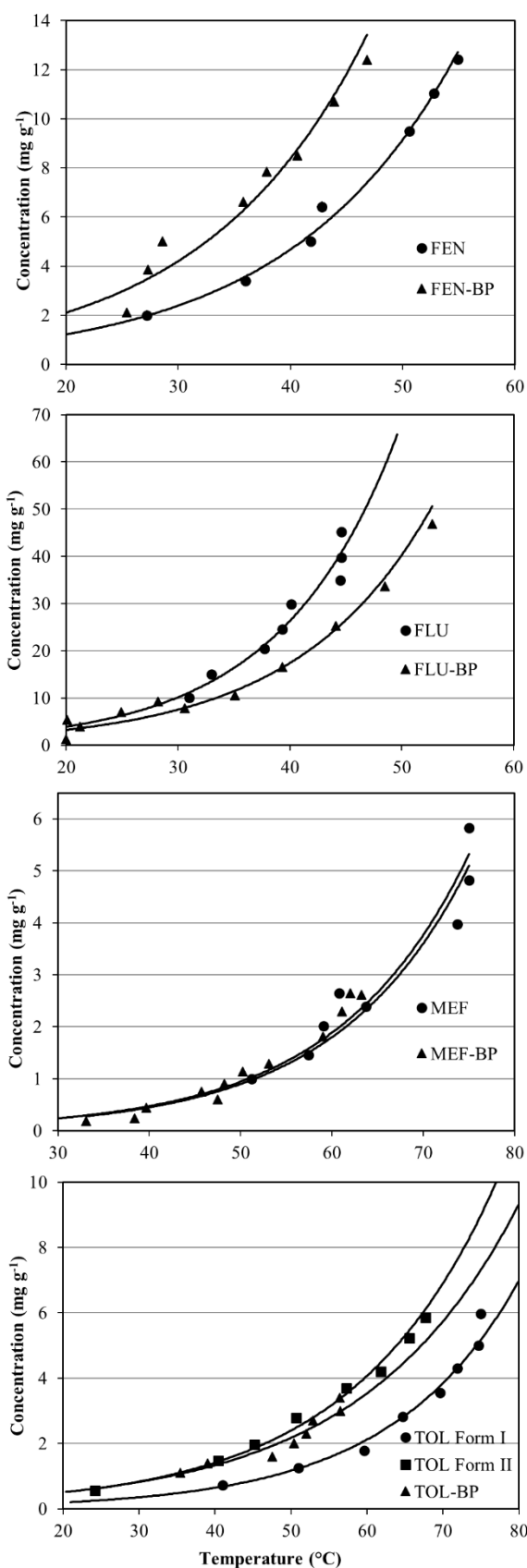
Fig. 8 Solubility curves for the APIs and co-crystals in isopropanol: water (1:1 v/v)

crystallised reproducibly here by a range of methods and characterised in terms of their thermal behaviour along with the determination of their key physical properties. The determination of these solid-form molecular structures and their physicochemical analysis add to the library of previously reported co-crystals discovered *en route* to enhancing important solid-state properties, such as thermal stability and solubility, of these NSAIDs.

In the pharmaceutical industry it is vitally important for APIs to display long term solid form stability. This is of particular note for polymorphic APIs, such as the fenamate family studied here, where phase transitions can occur due to heat and pressure changes, especially during secondary processing. It has been shown in this study that co-crystallisation enables these polymorphic transformations to be minimised, which is illustrated through the thermal investigations on four of the fenamic acid derivatives and their respective co-crystals. DSC measurements demonstrated that while the melting points of the co-crystals were lowered with respect to the APIs, the four fenamate co-crystals displayed no evidence of thermally induced phase transitions in contrast to the parent APIs. Although the APIs in this study are co-crystallised with the non-GRAS co-former 4,4'-bipyridine, it serves as a proof of concept model for future investigations into inhibition of polymorphism in APIs as solid form stability and selectivity has been achieved under the experimental conditions investigated here.

The stability of the reported co-crystals provides a robustness with respect to the crystallisation method used for their production. A variety of crystallisation methods, including rapid and controlled cooling, evaporative and grinding crystallisations, have all produced the desired co-crystals, in a single polymorphic form and reproducibly. This is of the utmost importance for large-scale production where available techniques and environmental control can be variable.

It is of particular value that co-crystallisation has been achieved through cooling methods as this is the most commonly used technique in industrial crystallisation at present. Additionally, co-crystallisation through liquid-assisted grinding, which has been demonstrated in this investigation, can be translated to a screw extrusion process on an industrial scale.[37] This offers environmental benefits through a significant or complete reduction in solvent use[38] and thus minimises the risk of potentially toxic residual solvent remaining in the end product.[39,40]

Turbidimetric measurements have provided solubility data of the APIs and their 4,4'-bipyridine co-crystals over a temperature range of 25-70 °C in an IPA/water solvent system. Characterising the solubility of starting materials and products is an early step in designing any cooling crystallisation process and is fundamental to the optimisation of scale-up to industrial crystallisation volumes. The data presented will be beneficial to the design and optimisation of future cooling crystallisation processes comprising these materials.

Acknowledgements

Notes and references

5 *a Department of Chemistry, University of Bath, Bath, BA2 7AY, UK; E-mail: c.c.wilson@bath.ac.uk, dyanne.cruickshank@uct.ac.za*
b Engineering and Physical Sciences Research Council (EPSRC) Centre for Innovative Manufacturing in Continuous Manufacturing and Crystallisation (CMAC), University of Bath, Bath, BA2 7AY, UK.

10 † Electronic Supplementary Information (ESI) available: [The CIF files (CCDC 1018667-1018669 have been deposited with the Cambridge Crystallographic Data Centre. A supporting information file has also been supplied with additional figures]. See DOI: 10.1039/b000000x/

1. V. López-Mejías, J. W. Kampf and A. J. Matzger, *J. Am. Chem. Soc.*, 15 2012, **134**, 9872-9875.

2. S. SeethaLekshmi and T. N. Guru Row, *Cryst. Growth Des.*, 2012, **12**, 4283-4289.

3. *V. R. R. Cunha, C. M. S. Izumi, P. A. D. Petersen, A. Magalhães, M. L. A. Temperini, H. M. Petrilli and V. R. L. Constantino, J. Phys. Chem.* 20 *B.*, 2014, **118**, 4333–4344.

4. V. López-Mejías, J. W. Kampf and A. J. Matzger, *J. Am. Chem. Soc.*, 2009, **131**, 4554-4555.

5. R. Thakuria, A, Delori, W. Jones, M. P. Lipert, L. Roy and N. Rodríguez-Hornedo, *Int. J. Pharm.*, 2013, **453**, 101-125.

25 6. K. S. Khomane, P. K. More, G. Raghavendra and A. K. Bansal, *Mol. Pharm.*, 2013, **10**, 631-639.

7. S. D. Clas, *Curr. Opin. Drug Discovery Dev.*, 2003, **6**, 550-560.

8. M. Maniruzzaman, M. M. Rana, J. S. Boateng, J. C. Mitchell and D. Douroumis, *Drug Dev. Ind. Pharm.*, 2013, **39**, 218-227.

30 9. D. T. Guranda and G. N. Gil'deeva, *Pharm. Chem. J.*, 2010, **44**, 22-28.

10. K. Wittering, J. King, L. H. Thomas and C. C. Wilson, *Crystals*, 2014, **4**, 123-140.

11. E. H. Lee, S. X. M. Boerrigter, A. C. F. Rumondor, S. P. Chamarthy 35 and S. R. Byrn, *Cryst. Growth Des.*, 2008, **8**, 91-97.

12. E. H. Lee, S. R. Byrn and M. T. Carvajal, *Pharm. Res.*, 2006, **23**, 2375-2380.

13. N. Schultheiss and A. Newman, *Cryst. Growth Des.*, 2009, **9**, 2950-2967.

40 14. L. Fang, S. Numajiri, D. Kobayashi, H. Ueda, K. Nakayama, H. Miyamae and Y. Morimoto, *J. Pharm. Sci.*, 2004, **93**, 144-154.

15. M. S. Fonari, E. V. Ganin, A. V. Vologzhanina, M. Yu. Antipin and V. Ch. Kravtsov, *Cryst. Growth Des.*, 2010, **10**, 3647-3656.

16. L. Fabian, N. Hamill, K. S. Eccles, H. A. Moynihan, A. R. Maguire, 45 L. McCausland and S. E. Lawrence, *Cryst. Growth Des.*, 2011, **11,** 3522-3528.

17. S. Aitipamula, A. B. H. Wong, P. S. Chow and R. B. H. Tan, *CrystEngComm*, 2014, **16**, 5793-5801.

18. P. Sanphui, G. Bolla and A. Nangia, *Cryst. Growth Des.*, 2012, **12**, 50 2023-2036.

19. S. Kumaresan, P. G. Seethalakshmi, P. Kumaradhas and B. Devipriya, *J. Mol. Struct.*, 2013, **1032**, 169-175.

20. Cambridge Structural Database, Ver. 5.35, November 2014

21. A. O. Surov, A. A. Simagina, N. G. Manin, L. G. Kuzmina, A. V. 55 Churakov and G. L. Perlovich, *Cryst. Growth Des.*, 2014, DOI: 10.1021/cg5012633.

22. A. Mukherjee and G. R. Desiraju, *Cryst. Growth Des.*, 2014, **14**, 1375-1385.

23. G. Li Destri, A. Marrazzo, A. Rescifina and F. Punzo, *J. Pharm. Sci.*, 60 2013, **102**, 73-83.

24. A. N. Saleemi, G. Steele, N. I Pedge, A. Freeman and Z. K. Nagy, *Int. J. Pharm.*, 2012, **430**, 56-64.

25. G. Sheldrick, *Acta Cryst. A*, 2008, **64**, 112-122.

26. A. L. Spek, *J. Appl. Crystallogr.*, 2003, **36**, 7-13.

65 27. Advantage (Software), version 5.5.3; TA Instruments: New Castle, DE, USA, 2013.

28. CrystalClear (Software), version 1.0.1.614: Avantium Pharmatech BV: Amsterdam, The Netherlands, 2013.

29. S. Romero, B. Escalera and P. Bustamante, *Int. J. Pharm.*, 1999, **178**, 70 193-202.

30. T. Umeda, N. Ohnishi, T. Yokoyama, T. Kuroda, Y. Kita, K. Kuroda, E. Tatsumi and Y. Matsuda, *Chem. Pharm. Bull.*, 1985, **33**, 2073 - 2078.

31. R. K. Gilpin and W. Zhou, *Vib. Spectrosc.*, 2005, **37**, 53-59.

75 32. A.V. Trask, W. D. S. Motherwell, and W. Jones, *Cryst. Growth Des.*, 2005, **5**, 1013–1021.

33. A. V. Trask, W. D. S. Motherwell and W. Jones, *Int. J. Pharm.*, 2006, **320**, 114-123.

34. N. J. Babu, P. Sanphui and A. Nangia, *Chem. Asian J.*, 2012, **7**, 2274– 80 2285.

35. M. D. Eddleston, R. Thakuria, B. J. Aldous and W. Jones, *J. Pharm. Sci.*, 2014, **103**, 2859-2864.

36. F. Kato, M. Otsuka and Y. Matsuda, *Int. J. Pharm.*, 2006, **321**, 18-26.

37. C. Medina, D. Daurio, K. Nagapudi and F. Alvarez-Nunez, *J. Pharm.* 85 *Sci.*, 2010, **99**, 4, 1693-1696.

38. S. L. James, C. J. Adams, C. Bolm, D. Braga, P. Collier, T. Friscic, F. Grepioni, K. D. M. Harris, G. Hyett, W. Jones, A. Krebs, J. Mack, L.Maini,d A G. Orpen, I. P. Parkin, W. C. Shearouse, J. W. Steed and D. C. Waddell, *Chem. Soc. Rev.*, 2012, **41**, 413–447.

90 39. A. Y. Lee, D. Erdemir and A. S. Myerson, *Annu. Rev. Chem. Biomol. Eng.*, 2011, **2**, 259-280.

40. H. G. Moradiya, M. T. Islam, S. Halsey, M. Maniruzzaman, B. Z. Chowdhry, M. J. Snowden and D. Douroumis, *CrystEngComm*, 2014, **16**, 3573 -3583.